The *Meloidogyne graminicola* effector Mg16820 is secreted in the apoplast and cytoplasm to suppress plant host defense responses

Diana Naalden[1], Annelies Haegeman[1,3], Janice de Almeida-Engler[2], Firehiwot Birhane Eshetu[1,4], Lander Bauters[1] and Godelieve Gheysen[1*].

[1] *Department of Biotechnology, Faculty of Bioscience Engineering, Ghent University, Coupure links 653, 9000 Ghent Belgium*
[2] *INRA, Université Côte d'Azur, CNRS, ISA, 06903, Sophia Antipolis, France*
[3] *Current address: Flanders Research Institute for Agriculture, Fisheries and Food (ILVO), Plant Sciences Unit, Caritasstraat 39, 9090 Melle, Belgium*
[4] *Current address: Department of Genetics, Forestry and Agricultural Biotechnology Institute (FABI), University of Pretoria, Pretoria 0002, South Africa*

* Corresponding author: godelieve.gheysen@ugent.be

Word count: 10 226

Key words: root-knot nematodes, parasitism, PAMP triggered immunity, effector triggered immunity, reactive oxygen species, *Oryza sativa*, *Nicotiana benthamiana*

Abstract

While invading roots, plant-parasitic nematodes secrete effectors to manipulate cellular regulation of the host to promote parasitism. The root-knot nematode *Meloidogyne graminicola* is one of the most damaging nematodes of rice. Here, we identified a novel effector of this nematode named Mg16820, expressed in the nematode subventral glands. We have localized the Mg16820 effector in the apoplast during the migration phase of the second-stage juvenile in rice roots. In addition, during early development of the feeding site, Mg16820 was localized in the giant cells where it accumulates in the cytoplasm and the nucleus. Using transient expression in *Nicotiana benthamiana* leaves, we have demonstrated that Mg16820 directed to the apoplast is able to suppress the flg22 induced reactive oxygen species production. On the other hand, expression of Mg16820 in the cytoplasm suppresses the R2/Avr2 and Mi-1.2 induced hypersensitive response. A potential target protein of Mg16820 identified with the yeast two-hybrid system is the dehydration-stress inducible protein 1 (DIP1). Bimolecular fluorescence complementation resulted in a strong signal in the nucleus. *DIP1* is described as an abscisic acid (ABA) responsive gene and ABA is involved in biotic and abiotic stress response. Our results demonstrate that Mg16820 is able to act in two cellular compartments as an immune suppressor and is targeting a protein involved in stress responses, therefore indicating an important role for this effector in parasitism.

Introduction

The root-knot nematode *Meloidogyne graminicola* is able to infect over 100 plant species including cereals, grasses and dicots, although the number of known dicot hosts is limited (Bridge *et al.,* 2005; Yik *et al.*, 1979). *M. graminicola* is best known as the most damaging root-knot nematode on the staple food rice and is responsible for yield losses between 17% to 32% (Kyndt *et al*., 2014). Pre-parasitic second-stage juveniles (J2s) invade in the root elongation region, migrate to the tip, turn and search for a suitable cell in the vascular cylinder to induce a specialized feeding site. This feeding site is formed by 5-8 highly active giant cells that arise by repeated nuclear division without cytokinesis (Kavitha *et al*., 2016; Kyndt *et al.*, 2014). When the nematode becomes sedentary, the parasitic J2 develops into a J3, J4 and finally an adult male or female with egg mass within 14-27 days, depending on environmental conditions (Kyndt *et al*., 2014; Mantelin *et al*., 2017).

To colonize the host, plant-parasitic nematodes have developed sophisticated methods to invade roots and change host cell regulation to support parasitism. Effectors are secreted from the glands into the host plant tissue, either in the apoplast or the cytoplasm. Secreted in the cytoplasm, the effector can interact there with receptors or other proteins or can be relocated to several other cell compartments like the nucleus or plasma membrane (Jaouannet & Rosso, 2013). Secreted in the apoplast, effectors may have a cell-wall degrading function or may interact with a receptor in the plasma membrane (Jaouannet & Rosso, 2013). Effectors may have a role in many pathways to induce a feeding site and to suppress the immune system of the plant. The plant's immune system is built in two layers (Jones & Dangl, 2006). The basal defense response recognizes slowly evolving microbial- or pathogen-associated molecular patterns (MAMPS or PAMPs) which are molecules common to many invaders. These molecules are recognized by surface pattern recognition receptors (PRRs) connected to the apoplast of plant cells, inducing a nonspecific defense response called the PAMP-triggered immunity (PTI). Nematode secretions and cuticle factors may be recognized as PAMPs (Abad *et al.*, 2003; Manosalva *et al.,* 2015). Due to the PTI response the plant becomes less susceptible and therefore nematodes evolved effectors to increase the susceptibility of the plant, the effector-triggered susceptibility (ETS). In the second layer of the immune system the effector can be recognized by the plant cell, inducing effector-triggered immunity (ETI). In response, nematodes have evolved effectors to suppress the second layer of defense as well. Finally, the ETI can lead to a local cell death, the hypersensitive response, which stops the development or kills the nematode.

The first nematode effector described by Smant *et al.* (1998) was identified as a β-1,4-endoglucanase, used by the nematode for degrading cellulose of plant cell walls. Now, many more effectors of plant parasitic nematodes have been identified but only a relatively small number has been functionally analyzed (Ali *et al*., 2017). Several potential effectors were found in the transcriptome of *M. graminicola* (Haegeman *et al*., 2013; Petitot *et al*., 2016). However, insight in their function is either based on predictions compared to homologs or the function remains unclear due to lack of known domains or well described homologs. Recently the first effector of *M. graminicola*, MgGPP, was functionally analyzed by Chen *et al.* (2017). This effector targets the endoplasmic reticulum (ER) and after N-glycosylation and C-terminal proteolysis, the effector is translocated to the nucleus. N-glycosylation of this effector is essential for the suppression of the Gpa2/RBP-1 induced hypersensitive response.

Here, we present the functional analysis of the *M. graminicola* Mg16820 protein which was identified as effector candidate by analysis of the data from Haegeman *et al.* (2013). However, Mg16820 was not included in that paper and therefore this is the first time this effector is presented. The coding sequence contains a predicted signal peptide, but no transmembrane domain, and no homologues in expressed sequence tag (EST) datasets of free-living nematodes were found during that study. In addition, the gene showed a high expression in the pre-parasitic second-stage juveniles. In this study, *in situ* hybridization was performed to analyze spatial expression of *Mg16820* in the nematode and the location of the effector was determined *in planta*. Finally, plant immune triggering assays were done and yeast-two-hybrid was performed to identify potential target proteins in rice.

Results

Mg16820 encodes a protein with a predicted size of 69 amino acids and is only found in root-knot nematodes

The open reading frame (ORF) of *Mg16820* contains 273 nucleotides (Figure S1), encoding a protein of 90 amino acids (Figure 1). The first 21 amino acids are predicted to function as an N-terminal secretion signal or signal peptide. When *Mg16820* was blasted against the *M. graminicola* genome (MGRAMBASE), we were not able to retrieve an identical hit. However a homologous sequence was retrieved with 72% protein identity. The major difference was detected in the N-terminal region coding for the predicted signal peptide, which was shorter compared to the cDNA sequence of *Mg16820*. No significant hits were found when *Mg16820* was blasted against the non-redundant protein and nucleotide databases for all organisms. The search for possible homologues was extended by performing a blast against fungal and oomycete genomes (FungiDB) and bacterial genomes (Microbial nucleotide blast on NCBI), but no hits were found. Additionally, some other genomes of plant parasitic nematodes were queried for homologues (*Bursaphelenchus xylophilus*, *Globodera pallida*, *M. incognita* and *M. hapla*). Only the genome of *M. incognita* contained two possible homologues (*Minc05708* and *Minc03663*). Both of them were predicted to have an N-

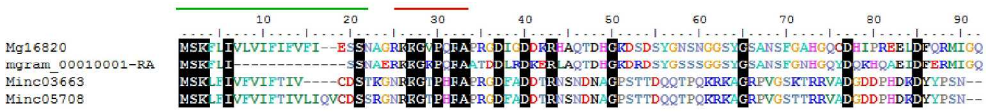

Figure 1: Alignment of the protein sequence of *Mg16820*, with DNA sequence obtained from MGRAMBASE and possible homologues (Minc05708 and Minc03663) in *M. incognita*. Green line indicates predicted signal peptide of Mg16820. Red line indicates the predicted NLS.

323x39mm (300 x 300 DPI)

terminal SP as well. Aligning all sequences shows that the 18 AA directly following the secretion signal are quite well conserved with only some additional aspartate and glycine residues conserved throughout the sequence. Using Wolf PSort, all 4 sequences (two sequences from *M. graminicola* and two from *M. incognita*) were predicted to have a nuclear localization once the putative secretion signal was cleaved. Using LOCALIZER, which specifically predicts effector localizations (Sperschneider *et al*., 2017), only the DNA sequence obtained from MGRAMBASE and the sequence of *Minc03663* predicted a nuclear localization. A predicted NLS was found ^{23}RKKGVPQRA^{31} just behind the SP, with a relative low activity (cut-off value 0.244). Both Minc03663 and Minc05708 contain an NLS with a higher activity as predicted with Mg16820 (0.900 and 0.667, respectively). In addition, the NLS was found at another location in the sequence, ^{37}KRKAGRPVGSK^{47} (Minc03663) and ^{40}KRKAGR^{45} (Minc05708). In the DNA sequence obtained from MGRAMBASE an NLS was found at ^{19}RAATDDLRDK^{28} with a cut-off value of 0.827.

Mg16820 is expressed in the subventral glands of the pre-parasitic juveniles

To determine if *Mg16820* is expressed in the pharyngeal glands of pre-parasitic J2s, *in situ* hybridization experiments were performed. A strong signal was visible in the subventral glands of the nematodes when hybridized with the antisense probe (Figure 2 A). As negative control for the hybridization, a sense probe against *Mg9152* was used, that did not result in a signal (Figure 2 B).

Mg16820 is secreted during the migratory and early sedentary stage

To determine if and where the effector Mg16820 is secreted in the host plant, immunolocalization was applied to rice gall sections containing nematodes at 1, 3, 5, 7 and 10 days post inoculation (dai). At 1 dai nematodes are at the migratory stage in or near the root tip. Mg16820 was detected in the head region, the subventral pharyngeal glands of the nematode or in the apoplast along the plant tissue at the anterior part of the nematode (Figure 3 A-F). At early gall development Mg16820 was detected inside the young giant cells (3 and 5 dai) (Figure 3 G-N). The effector was found in the cytoplasm and in the nuclei most likely being excluded from the nucleoli (Figure 3 I-N). At 7 dai the Mg16820 signal was still observed in the galls but at 10 dai Mg16820 was undetectable (Figure S2). Sections incubated with the pre-immune serum or only with secondary antibody did not show any green fluorescence indicating that the antibody was specifically detecting the Mg16820 effector protein (Figure S2).

Mg16820 is localized in the cytoplasm and nucleus when expressed in *N. benthamiana* leaves

The subcellular localization of Mg16820 was also determined by transient expression in *N. benthamiana* leaves. To mimic the secretion of Mg16820 in the cytoplasm *Mg16820* was expressed without signal peptide. Several constructs were used with *Mg16820* fused to *eGFP* and *eRFP* both N- and C-terminally, giving similar results, namely Mg16820 was detected in the nucleus and in the cytoplasm (Figure 4 B). Mg16820 exclusion from the nucleoli as seen during immuno-detection assays was not observed. To mimic the secretion of Mg16820 in the apoplast *Mg16820* was expressed with signal peptide (*SPMg16820*::GFP). A relatively weak signal was observed in the cell surroundings. Although it could not be confirmed Mg16820 was actually located in the apoplast, the lack of signal in the nucleus indicates that the nematode signal peptide is functional in plant cells and Mg16820 was transported to the apoplast (Figure 4 C).

Mg16820 directed into the apoplast suppresses the flg22 induced ROS production

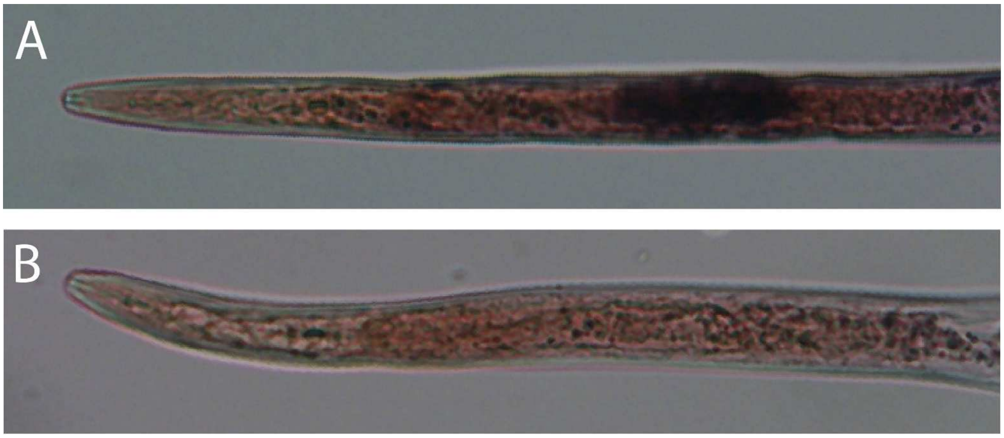

Figure 2: *In situ* hybridization of *M. graminicola* pre-parasitic second stage juveniles. A: Antisense probe of *Mg16820*. B: Sense probe (negative control; putative effector *Mg9152*).

300x129mm (300 x 300 DPI)

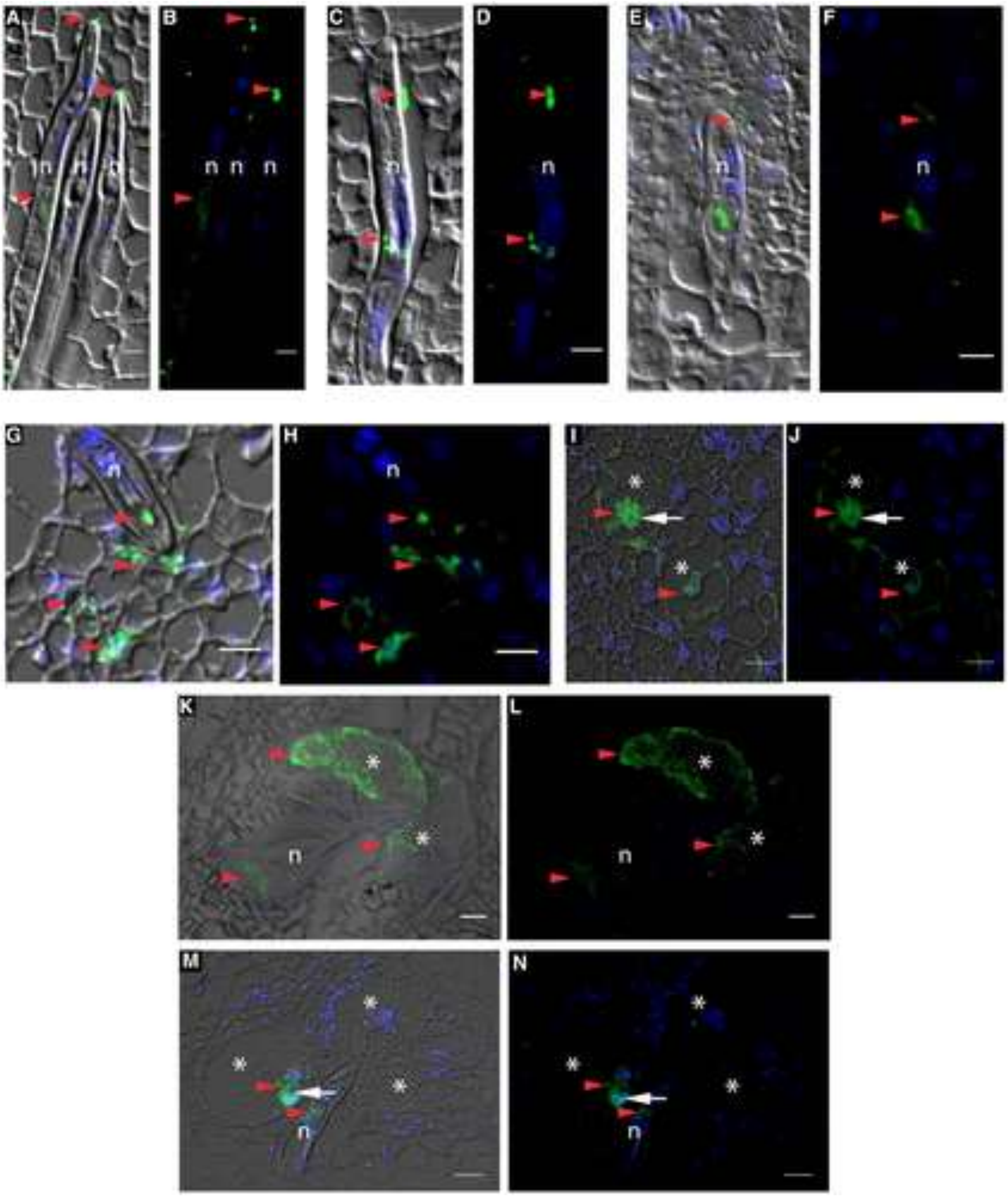

Figure 3: Immunolocalization of Mg16820 secreted by M. graminicola in rice. A-F: Immunolocalization of Mg16820 during the migratory phase of the nematodes (1 dai). A and B: Secretion of Mg16820 (green fluorescence) by two nematodes with signal seen in the subventral glands in one juvenile nematode. C and D: Migrating nematode with Mg16820 signal at the anterior part, along the body in the plant apoplasm and in the nematode body. E and F: Signal at the anterior part and inside the nematode body. G-J: Immunolocalization of Mg16820 in the feeding sites 3 dai. G and H: Secretion of Mg16820 in the plant tissue prior to giant cell development. I and J: Young giant cells showing signal in the cytoplasm and in the nuclei apparently excluded from the nucleoli. K-N: Immunolocalization of Mg16820 during feeding site development (5 dai). K and L: Accumulation of Mg16820 in the cytoplasm of giant cells. M and N: Young giant cells showing signal in the cytoplasm and nucleus apparently excluding the nucleoli. Grey pictures = DIC, DAPI and GFP overlay, black pictures = DAPI and GFP overlay, n = nematode, g = glands, asterisks = giant cells, red arrowheads = Mg16820, blue colour = nuclei, white arrow =nucleolus. Scale bars A-J = 10 µM, K-N= 20 µM.

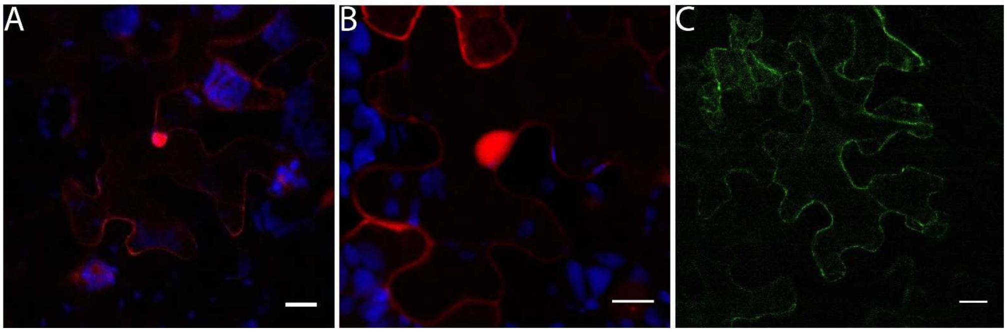

Figure 4: Subcellular localization of Mg16820 after transient expression in *N. benthamiana* leaves. A: localization of free RFP in the cytoplasm and nucleus. B: Localization of Mg16820::RFP in the cytoplasm and nucleus. C: Localization of SPMg16820::GFP. Scale bar: A: 20 μM, B: 10 μM, C: 20 μM.

361x118mm (300 x 300 DPI)

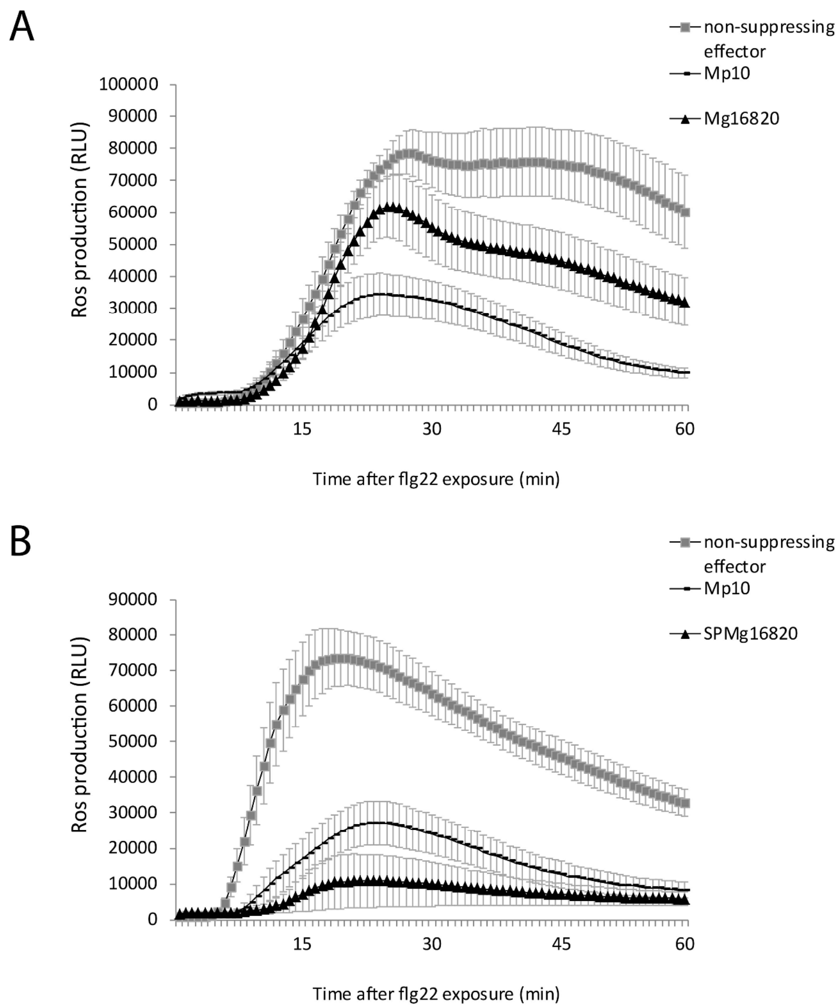

Figure 5: Suppression assay of flg22 induced ROS production in *N. benthamiana* with Mg16820. A: Weak suppression of ROS with Mg16820 located in the cytoplasm compared to the non-suppressing effector Mg03015. Mp10 is used as positive control suppressing ROS. B: Very strong suppression with Mg16820 localized in the apoplasm (SPMg16820). The effector Mg03015 with signal peptide was used as negative control not suppressing ROS. Mp10 is used as positive control. Bars indicate standard error.

289x298mm (300 x 300 DPI)

To investigate if Mg16820 may have a role in the suppression of the early immune response of the plant, a luminol based assay was used to measure the effect of *Mg16820* expression on ROS production after PTI induction by flg22. When *Mg16820* was expressed without signal peptide, and therefore the protein was present in the cytoplasm, the suppression was variable between the different assays. In some cases no suppression was seen, while around half of the assays indicated a weak but significant suppression (Figure 5 A). ROS production was dramatically decreased when Mg16820 was translocated to the apoplast of the cell (Figure 5 B). This suppression was consistent in all assays.

Mg16820 directed into the cytoplasm suppresses the R2/Avr2 and Mi-1.2^{T557S}induced hypersensitive response

Effector triggered immunity (ETI) assays were performed by co-infiltration of several combinations of avirulence and resistance genes to induce a hypersensitive response (HR). These constructs were combined with *Mg16820* with or without signal peptide to investigate if the effector could interfere with ETI. Mg16820 with signal peptide did not result in suppression in any of the tested HR pairs. Mg16820 localized in the cytoplasm was able to suppress two different pathways: the pathway induced by the combination of *Solanum demissum* R2 and *Phytophthora infestans* Avr2 and by the auto-activation tomato resistance gene *Mi-1.2^{T557S}* (Figure 6). The suppression of Mi-1.2 induced HR was stronger, more consistent and the percentage of suppressed spots was more compared to the R2/Avr2 induced HR. Mg16820 was not able to suppress both pathways when tagged with either HA and GFP. Several other ETI pairs were tested, but they did not result in suppression of the HR (Table 1).

A potential target protein of Mg16820 is the dehydration-stress inducible protein 1 (DIP1)

To identify interactors of Mg16820, a yeast two-hybrid screen was performed with a cDNA library from infected rice tissues. This resulted in one potential interactor which was identified as the dehydration-stress inducible protein 1 (DIP1; LOC_Os05g34070.1). The interaction with the isolated *GAL4*-DNA-activation-domain::*DIP1* and *GAL4*-DNA-binding-domain::*Mg16820* resulted in a faint blue coloring in the X-gal assay. Cell growth was seen on the TLH-selection medium, but not on the TLU-selection medium and therefore this interaction is considered as weak. The same assay with the complete *DIP1* fused N-terminally to the *GAL4* DNA activation domain did not result in blue color or growth on the –TLU-selection medium (Figure 7).

To determine if interaction between effector Mg16820 and the complete DIP1 protein could be proven *in planta*, a bimolecular fluorescence complementation was performed using transient expression in *N. benthamiana* leaves. As negative control the putative effector Mg03015 was used with the same plant subcellular localization as Mg16820 and with similar size. RT-PCR showed a similar expression for *Mg16820* and *Mg03015* (Figure S3). YFP signal could be detected in leaves infiltrated with *Mg16820* and *DIP1* (Figure 8 B & C), mostly in the nucleus but excluded from the nucleolus, while *Mg03015* co-infiltrated with *DIP1* did not result in any signal (Figure 8 A).

Table 1: Effector triggered immunity suppression assays in *N. benthamiana* with effector Mg16820 with and without signal peptide.

	Mg16820	SPMg16820	EV	GFP
Cf-4/Avr4	-	-	-	-
Cf-9/Avr9	-	-	-	-
INF1	-	-	-	-
Mi-1.2^{TSS7S}	+	-	-	-
Gpa2/RBP-1	-	nt	-	-
R2/Avr2	+	nt	-	-
R3a/Avr3a	-	nt	-	-

-: No suppression, +: suppression, nt: not tested. Each negative assay was done at least twice with 19-20 plants with 2 leaves per plant, each positive assay was performed at least three times with 19-20 plants with 2 leaves per plant.

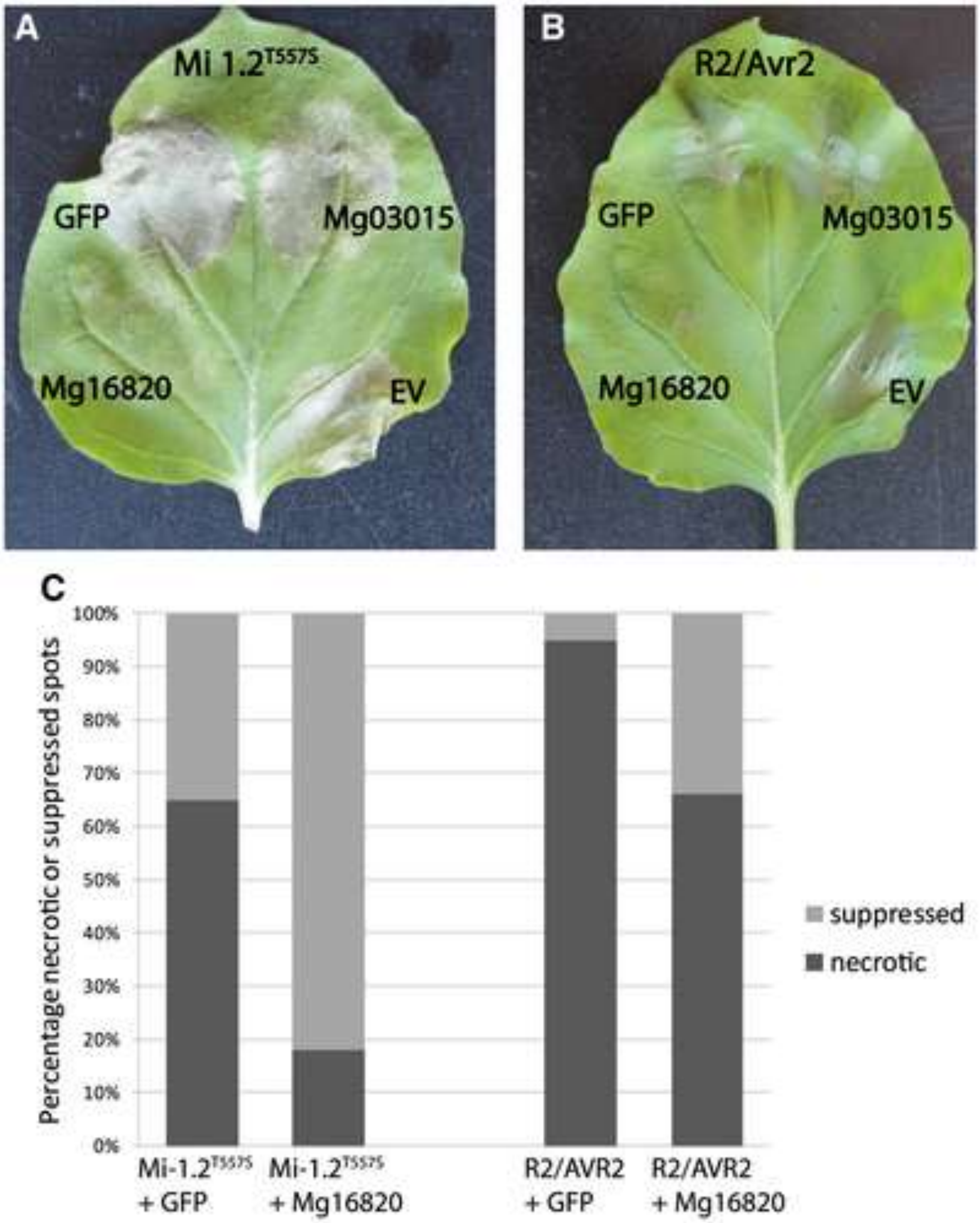

Figure 6: Effector-triggered immunity (ETI) suppression assays in *Nicotiana benthamiana* with effector Mg16820 suppressing two ETI pathways. (A) Suppression of the Mi-1.2^{T557S}-induced hypersensitive response (HR) by Mg16820 without signal peptide, targeted to the cytoplasm. The controls empty vector (EV), green fluorescent protein (GFP) and non-suppressing effector Mg03015 of *Meloidogyne graminicola* did not result in suppression. (B) Suppression of the R2/Avr2-induced HR by Mg16820 localized in the cytoplasm with the same controls as in (A). (C) Percentage of necrotic and suppressed spots with *Mi-1.*2^{T557S} and R2/Avr2 co-infiltrated with *Mg16820*.

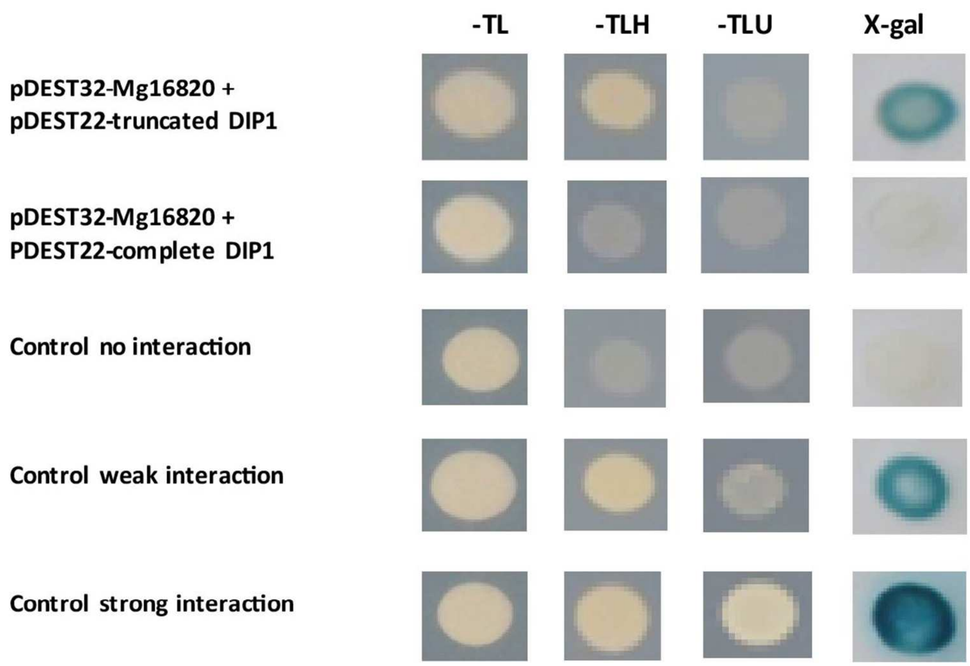

Figure 7: Yeast two-hybrid co-transformation assay with *GAL4*-DNA-binding-domain::*Mg16820* and *GAL4*-DNA-activation-domain::*DIP1*. Interaction was tested by using medium lacking the auxotrophic markers histidine (-TLH) and uracil (-TLU). To test β-galactosidase activity the X-gal substrate was used. The truncated DIP1 isolated from the library showed a weak interaction with Mg16820, while the complete DIP1 sequence did not show interaction in the Y2H-assay.

106x76mm (300 x 300 DPI)

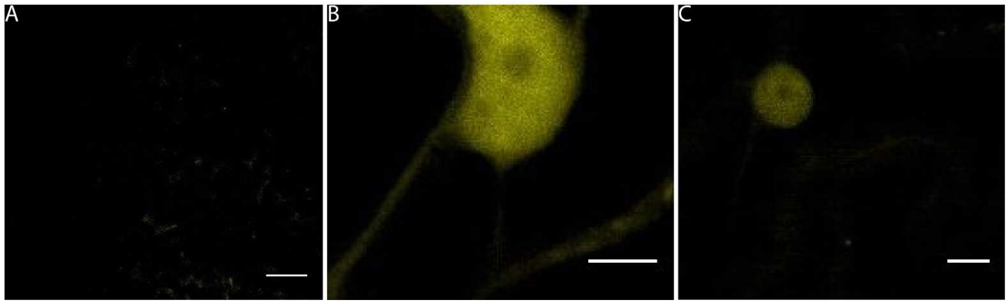

Figure 8: Bimolecular fluorescence complementation assay with Mg16820 and DIP1 in *N. benthamiana* leaves. YFP signal was seen in the nucleus with exclusion of the nucleolus. A: negative control *YFPc::Mg03015* and *YFPn::DIP1* with infiltration OD600 of 0.3. B: YFP signal with infiltration of *YFPc::Mg16820* and *YFPn::DIP1* in OD600 of 0.3. C YFP signal with infiltration of *YFPc::Mg16820* and *YFPn::DIP1* in OD600 of 0.1. Scale bars = A: 40 μM, B: 5 μM, C: 10 μM.

545x163mm (300 x 300 DPI)

Discussion

We performed a functional analysis of the *M. graminicola* effector Mg16820, which was identified by 454 sequencing of the transcriptome of second-stage pre-parasitic juveniles (contig 016820; method described by Haegeman *et al.* (2013)). In this study, we provide evidence that Mg16820 can be considered as an effector. The coding sequence of *Mg16820* includes a predicted signal peptide. Remarkable is the lack of a complete signal peptide in the genomic sequence found in the *M. graminicola* genomics resource database. Because the two potential homologs found in the genome database of *M. incognita* do have a predicted signal peptide, the *M. graminicola* genomic sequence might contain an assembly error. Most likely the conserved part plays a more important role in the function of the protein. Besides the well conserved N-terminal part, the C-terminus only shows some conserved aspartate and glycine residues. Possibly, these residues are essential for the function and protein folding. No homologs were detected in either the genome or transcriptome of other plant parasitic nematodes besides *M. graminicola* and *M. incognita*. It is likely the gene undergoes diversifying selection under pressure of the host immune system (Hewezi & Baum, 2013).

The expression of *Mg16820* in the subventral glands of the nematode was confirmed with *in situ* hybridization. The subventral glands are mainly active during the pre-parasitic and migratory life stages, in contrast to the dorsal gland that becomes active during sedentarization when the giant cells are induced (Davis *et al*., 2000). *Mg16820* is highly expressed by the pre-parasitic J2s (Petitot *et al.,* 2016). In the migratory stage (2 dai), the gene is still expressed but 4 times lower, which is further decreased at 4 dai and at 8 dai the expression is close to zero (Figure S4; Petitot *et al.,* 2016). This indicates that Mg16820 has a role in the early stages of parasitism.

Immunolocalization confirmed the expression and secretion of *Mg16820* in the early stage of parasitism. During the migratory stage *M. graminicola* juveniles move intercellularly (Mantelin *et al.*, 2017) and secretion of Mg16820 was observed in the apoplast. In addition, during early giant cell development Mg16820 was secreted in the cytoplasm and targeted to the nuclei as well. Most likely the nematode injects Mg16820 directly in the plant cell when initiating the giant cells, since our results showed a clear distinction of localization in either the apoplast or cytoplasm. Therefore, the role of Mg16820 during development of the feeding site is clearly located in the cytoplasm or nucleus. Localization in the nucleus might indicate a role in the transcriptional regulation in the plant cell (Jaouannet & Rosso, 2013).

However, the molecular size of Mg16820 (7.5 kDa without signal peptide) is very small and most likely the effector is just diffusing towards the nucleus since even molecules larger than 60 kDa can diffuse through the nuclear pore (Wang & Brattain, 2007). Even fused to eGFP, Mg16820 is smaller than 60kDa and although the effector was predicted to have a nuclear localization, the effector does not seem to be translocated effectively to the nucleus since the signal is similar in strength in the cytoplasm. This was observed in both the immunolocalization and the subcellular localization assay. However, some contradictory results were observed concerning Mg16820 localization in the nucleoli. With immunolocalization Mg16820 was excluded from the nucleoli, while with the subcellular localization the nucleoli could not be distinguished. The reason for this is unclear but the subcellular localization might show an artefact, related to the GFP tag on Mg16820, which is further discussed later.

The ability of *M. graminicola* to strongly suppress rice defense has been shown before by the analysis of defense gene expression (Ji *et al.*, 2015). We tested whether Mg16820 has a role in suppression of the plant immune system. The immune response assays in this study show the capacity of the effector as immune suppressor in both apoplast and cytoplasm. ROS production was measured to gain insight in the effect of Mg16820 in the apoplast. ROS are signaling molecules triggering PTI and ETI responses which subsequently result in more ROS production (Jwa & Hwang, 2017). ROS can negatively affect the pathogen because it can damage the nematode directly, strengthen the cell wall by cross-linking cell wall polymers, it induces defense signals and regulates cell death responses (Torres *et al*., 2006). The strong suppression of ROS production accomplished by this effector when it is present in the apoplast benefits the nematode. It remains unclear which mechanism is responsible for the Mg16820 mediated suppression of the flg22 induced ROS production. Possibly, Mg16820 works on the receptors or enzymes embedded in the plasma membrane to reduce the ROS response (Jwa & Hwang, 2017). For example, respiratory burst oxidase homologs (RBOHs) are an important group of enzymes in plants, responsible for electron transfer from cytosolic NADPH or FAD to oxygen present in the apoplast to form O_2^-, which is subsequently converted to H_2O_2 (Qi *et al*., 2017). Recently the *M. graminicola* effector MgM0237 targeting the cytoplasm was shown to be able to suppress the PTI response in *N. benthamiana* (Chen *et al*., 2018). When Mg16820 was present in the cytoplasm, ROS was not consistently suppressed and when suppression was observed, this was very weak. The assay is in general quite variable as also observed with the positive control Mp10, which resulted in variable levels of suppression. Therefore very weak suppression might not have been detected during each assay. However, variable cell breakdown due to the ROS may release Mg16820 in the apoplast, possibly resulting in a weak suppression. Therefore, most likely Mg16820 is not able to suppress the PTI response when it is present in the cytoplasm.

The ETI response can lead to an HR that causes rapid cell death of plant tissue around the pathogen putting the development of the pathogen on hold (Jones & Dangl, 2006). Therefore nematodes need to suppress this secondary layer of plant defense. The role of several effectors in ETI suppression has been confirmed (Ali *et al*., 2017) including the *M. graminicola* effector MgGPP that is able to suppress the Gpa2/ RBP-1 induced cell death (Chen *et al*., 2017). Based on our experiments Mg16820 is able to interfere with at least two different ETI pathways when present in the cytoplasm. Mg16820suppresses the *Solanum demissum* R2 and *Phytophthora infestans* Avr2 induced HR pathway and the auto-activation tomato resistance gene *Mi-1.2*^{T557S} induced HR pathway. The suppression of multiple ETI pathways by one effector has been observed for other nematode effectors as well. Msp40 secreted by *M. incognita* was able to prevent the Bax-triggered and R3a/Avr3a induced cell death when transiently the cytoplasm of *N. benthamiana* leaves. In addition, Msp40 was able to suppress callose deposition and the expression of genes related to the elf18 triggered PTI immune response. Like Mg16820, Msp40 was able to suppress both PTI and multiple ETI pathways (Niu *et al*., 2016). However, in contrast with Mg16820 the different activities of Msp40 appeared in the same cell compartment, the nuclei and cytoplasm, while Mg16820 works in the apoplast as well as in the cytoplasm. The *G. rostochiensis* effector GrUBCEP12 with and without signal peptide was able to suppress several elicitor induced cell death pathways (Ali *et al*., 2015). Although it was not confirmed by subcellular localization that the effector GrUBCEP12 indeed was transported to the apoplast at least it was confirmed that this effector works on several HR pathways. In addition, the effector MiSGCR1 secreted by *M. incognita* is able to suppress the AvrPto (*Pseudomonas syringae*) and NPP1 (*Phytophthora parasitica*) induced HR (Nguyen *et al.,* 2018). Interestingly, similarly to Mg16820, this effector was not able to suppress the HR when fused to GFP.

It was hypothesized this is probably an effect of misfolding of the fused protein or physical interference of the GFP protein with the binding of the effector to its target (Nguyen *et al*., 2018).

The Mi-1.2^{T557S} and R2/Avr2 induced hypersensitive response pathways may overlap and Mg16820 could interact with a target protein which is involved in both pathways. A yeast two-hybrid assay was performed to find a target protein in rice and our data suggest an interaction with the dehydration-stress inducible protein 1 (DIP1). Although the complete DIP1 protein did not show interaction in the yeast two-hybrid assay, we continued to perform a bimolecular fluorescence complementation assay because the truncated part isolated from the yeast two-hybrid library, comprises almost the complete sequence except that the start codon is missing. We could detect an interaction between Mg16820 and DIP1 *in planta* with bimolecular fluorescence complementation. This might be because the interaction was tested in plant cells instead of yeast and/or because of the difference in fused tags that may not interfere in the bimolecular fluorescence complementation technique.

In maize, DIP1 is an important component in the rab17 pathway, induced by the phytohormone ABA under influence of drought stress (Saleh *et al*., 2006). In rice the homolog of *rab17* is called *rab21* (Vilardell *et al*., 1990). Although it is not known if the rab21 pathway is involved in the HR pathways tested in this study, we can speculate that interaction between DIP1 and Mg16820 changes the expression of *rab21,* influencing the immune response. In galls, expression of *rab21* was downregulated at 3 dai while at 7 dai the expression was upregulated. In giant cells *rab21* was upregulated at both 7 and 14 dai (Ji *et al*., 2013) but the expression level at 3 dai was not determined. An increased expression of *DIP1* was observed in the gall tissue at 7 dai, but not at 3 dai. In the giant cells at 7 and 14 dai the expression level was similar compared to non-infected tissue. Plant response to pathogens is regulated by a complex network of phytohormone signaling and pathogens attempt to interfere with these pathways (Denancé *et al*., 2013). ABA is related to abiotic stresses, but its role in biotic stresses like pathogen attack becomes more understood (Lievens *et al.*, 2017). For example, it has been shown that ABA plays a direct role in regulation of resistance protein activity (Denancé *et al*., 2013). However, the role ABA plays differs between the different plant-pathogen interactions (Asselbergh *et al*., 2008). In rice, galls induced by *M. graminicola* show a twofold increased ABA level at 3 dai, while at 7 dai the ABA level is still increased but lower than at 3 dai. Application of ABA as well as of an ABA biosynthesis promotes susceptibility of rice to *M. graminicola* indicating a complex role for ABA in this plant-nematode relation (Kyndt *et al*., 2017). The ABA level in the host during the migratory stage of the nematode is not known. We should note that DIP1 is not present in the apoplast, but moves during drought stress from the cytoplasm to the nucleus (Saleh *et al*., 2006). Possibly Mg16820 is able to interfere with two different mechanisms to suppress the immune system of the plant. Alternatively Mg16820 works in the apoplast and in the cytoplasm by interacting with a component important in the ROS defense signaling which is part of both the PTI and ETI response.

In summary, we identified, localized and functionally analyzed the effector Mg16820 secreted by the root-knot nematode *M. graminicola*. To our knowledge this is the first effector published which is proven to be secreted in both the apoplast and the cytoplasm of giant cells during the early stages of parasitism and has immune suppressing capacities in both cell compartments. The mechanism behind the suppression of both the PTI and ETI response at two different subcellular localizations is not understood and needs further studies. In addition, DIP1 was identified as a potential target protein and due to the role in ABA response, further studies on this interaction may provide more insight in the molecular mechanism of plant parasitism.

Experimental Procedures

Nematode culture

Nematode cultures were obtained by inoculating pre-parasitic second-stage juveniles (J2) of *M. graminicola* (isolate from Philippines, Batangas) on rice plants or the grass *Echinocloa crus-galli* grown in universal soil (Structural, type 1, Belgium; mire, garden peat and mixed nutrients), which were then incubated for three months at 28°C with light/dark cycles of 16 hrs/8 hrs. To extract pre-parasitic J2s the infected roots were washed with tap water and cut in small pieces of circa 0.5 mm to open the galls. Nematodes were collected for 3 to 7 days using a modified Baermann method (Baermann, 1917).

Plant growth conditions

Nicotiana benthamiana seeds were germinated in moist universal soil (mire, garden peat and mixed nutrients) at 27°C and one week old individual plantlets were transferred to pots (diameter 15 cm) with the same soil and provided once directly after transferring with a commercial plant nutrient solution (Substral, NUTRI+MAX universal, 15 mL/10 L water). The plantlets were grown for 5-6 weeks at 27°C with light/dark cycles of 16 hrs/8 hrs. At least one day before infiltration the plants were transferred to room temperature (RT) and exposed to natural light for acclimatization. After infiltration the plants were kept at RT.

Oryza sativa cv. Nipponbare seeds were germinated on wet filter paper in the dark for 5 days at 30°C and then transferred to SAP (mixture of 0.7 g superabsorbent polymer (Aquaperla) per 1 kg and white sand) filled PVC tubes (Reversat & Boyer, 1999). The plantlets were grown for another 9 days at 27°C with light/dark cycles of 16 hrs/8 hrs before infection. The plantlets were provided 3 times a week with 10 mL Hoagland solution (Hoagland & Arnon, 1950) added directly to the tubes.

Sequence analysis

The effector *Mg16820* was identified using 454 sequencing of mRNA of pre-parasitic J2s (contig16820; method described in Haegeman *et al.,* 2013 but *Mg16820* was not described in that paper). Prediction of the signal peptide was performed by using SignalP 4.0 (http://www.cbs.dtu.dk/services/SignalP/). Prediction on cellular localization was done using Wolf PSort (https://wolfpsort.hgc.jp) and LOCALIZER (http://localizer.csiro.au; Sperschneider *et al.*, 2017). Prediction of the presence and localization of a nuclear localization signal was performed with SeqNLS (Lin *et al.*, 2012). The coding region of *Mg16820* was blasted using default parameters with a cut off value of 50 (bitscore) against the *M. graminicola* genomics resource database (MGRAMBASE; http://insilico.iari.res.in/mgram/), the non-redundant protein and nucleotide databases for all organisms of the National Center for Biotechnology Information (NCBI), fungal and oomycete genomes (FungiDB; http://fungidb.org/fungidb/) and bacterial genomes (Microbial nucleotide blast on NCBI), and the four genomic datasets of plant parasitic nematodes *Bursaphelenchus xylophilus*, *Globodera pallida*, *M. incognita* and *M. hapla.* In addition, a BLAST was done against the online *Meloidogyne* genomic resources database (INRA; http://meloidogyne.inra.fr/; (Blanc-Mathieu *et al.*, 2017)). The alignment of the predicted protein was made using the ClustalW multiple alignment algorithm in Bioedit sequence alignment editor.

Cloning *Mg16820* in different vectors

The full-length coding sequence of effector *Mg16820* was PCR amplified from *M. graminicola* J2 cDNA using gene specific primers (Mg16820-F-FL and Mg16820-R-FL; All primers are listed in Table S1) designed to the untranslated regions and ligated into the pGEM-T easy vector (Promega). PCR was performed using VWR® Taq DNA-polymerase with 30 cycles of 58°C annealing temperature and 1 min. elongation time. The PCR product was purified according to the manufacturer's instructions (QIAquick PCR Purification Kit) and was ligated in the pGEM-T vector according to the manufacturer's protocol (Promega). The plasmid was transformed into *E. coli* (DH5-α or Top10) using heat shock treatment (42 sec. on 42°C, incubation 2 min on ice and recovery for 1.5 hrs shaking on 200 rpm at 37°C) and grown overnight at 37°C on solid Luria-Bertani (LB) broth medium with 25 μ g/mL carbenicillin. Colony PCR was performed to confirm construct presence and selected colonies were grown overnight in liquid LB with the appropriate antibiotics at 37°C. Plasmids were isolated (GeneJET Plasmid Miniprep Kit, Fermentas) and verified by sequencing. This construct was used as template to fuse the effector sequence to attb sites and to ligate in the Gateway® pDONR™221 vector (Thermo Fischer Scientific). The effector was cloned with start and/or stop codon and with and without its native signal peptide using Mg16820-attb1, Mg16820-attb1+start, Mg16820-SP-attb1 or Mg16820-SP-attb1+start as forward primer and Mg16820-attb2 or Mg16820-attb2+stop as reverse primer. PCR product was amplified in 2 subsequent PCRs. In the first step gene specific primers were used in 20 μL PCR mix with annealing temperature of 45°C (5 cycles) followed by 54 °C and (15 cycles). In the second step 3 μL was taken from this PCR mix and used in 17 μL fresh PCR mix using the primer M-13-F and M-13-R using the same program as described above. Ligation reactions (LR Clonase ™II, Thermo Fisher Scientific) were performed to bring the *Mg16820* coding sequence to the appropriate destination vectors (pk7WG2, pk7FWG2, pk7WGF2, pH7RWG2, pH7WGR2, pDEST32, pDEST22 and pCL113). The same approach was followed for cloning the negative control, the pioneer putative effector *Mg03015* (contig03015; Haegeman *et al.,* 2013). This putative effector was chosen as negative control because it has a similar protein size and subcellular localization in *N. benthamiana* as Mg16820, but is not related in protein sequence. In addition, Mg03015 does not play a role in immune suppression in the assays presented in this research and therefore could be used as negative control. *Mg03015* was cloned in pGEM-T easy vector using primer pair Mg03015-F-FL and Mg03015-R-FL. *Mg03015* was cloned in pDONR™221 with start and stop codon and with and without its native signal peptide into the destination vector pk7WG2, using primers Mg03015-attb1 +start, Mg03015-SP-attb1 as forward primer and Mg03015-attb2 or Mg03015-attb2+stop as reverse primer. *Mg03015* was cloned without native signal peptide and with stop codon in pDONR™221 and subsequently in pCL113. All constructs were sequenced to check for mutations (LGC genomics, Berlin) and destination vectors were screened for frameshifts before being used in the experiments (sequencing primers listed in Table S1). Constructs were either transformed in yeast strain MaV203 for the yeast two-hybrid assay (protocol Invitrogen) or Agrobacterium strain GV3101 for agro-infiltration [Freeze–thaw method of Holsters *et al*. (1978)].

***In situ* hybridization**

A 316 bp PCR product was obtained from the pGEM-T- *Mg16820* construct using gene specific primers (Mg16820-F-ISH, Mg16820-R-ISH). Single strand DNA probes were amplified using Mg16820-R-ISH primer in an asymmetric PCR with digoxigenin (DIG)-labelled dNTPs (Roche, Mannheim, Germany). Because the in situ hybridization was part of a high throughput experiment, only one negative control was used for the reaction instead of for each effector separately. As a negative control for the *in situ* hybridization a sense probe of the putative effector Mg9152 was used (Contig9152; database Haegeman *et al*., 2013). A 333 bp PCR product was obtained using primer pair Mg9152-F-ISH, Mg9152-R-ISH with pGEMT-*Mg9152* as template. Single strand DNA probes using primer Mg9152-F-ISH were amplified as described above. Pre-parasitic J2s were fixed in 2% paraformaldehyde overnight at 4°C, cut in pieces and permeabilized with proteinase K. Nematodes were hybridized with the DIG labelled sense or antisense probes that were detected with an anti-digoxigenin alkaline phosphatase conjugated antibody following the protocol of de Boer *et al.* (1998) with the hybridization temperature adapted to 47°C to increase probe binding to the template.

Peptide synthesis and antibody purification

Peptides for immunolocalization were designed according to the Thermofisher Scientific Antigen profiler. To avoid background, the designed peptides were blasted against the rice genome annotation project (http://rice.plantbiology.msu.edu) and NCBI Basic Local Alignment Search Tool (https://blast.ncbi.nlm.nih.gov/Blast.cgi) to check for potential similarities between the selected peptide sequences and host plant proteins. Two rabbits were immunized with two synthetic peptides: KRHAQTDHGKDSDS and HIPREELDFQRMIGQ (Thermofisher Scientific). Primary antibodies were purified from the rabbit with the lowest background (Thermo Fisher Scientific).

Fixation and embedding of galls

Two week old rice plantlets in SAP were infected with freshly hatched pre-parasitic J2s. At 24 hrs after inoculation the plantlets were washed briefly and transferred to clean SAP to avoid nematode infection at later time points, thus synchronizing the infection. To obtain galls, the infected root systems were collected at 1, 2, 3, 5, 7 and 10 dai, washed thoroughly with tap water and galls were then dissected from the roots and placed in fixative [4% formaldehyde in 50 mM piperazine-N,N'-bis (ethanesulfonic acid) (PIPES) buffer, pH 7.2]. Galls were vacuum treated for 30 min to remove air from the tissue, transferred to fresh fixative in cell strainers and placed at 4°C shaking gently for 2-10 days depending on the gall size. Fixation and embedding were further performed essentially as described by de Almeida Engler *et al.* (2004) and Kronenberger *et al*. (1993). Galls were then sectioned to 5 µm using an ultra-microtome and placed on poly-l-lysine coated slides as described by Vieira *et al.* (2011).

Immunolocalization of Mg16820

The immunolocalization was performed according to de Almeida Engler *et al*. (2004) and Vieira *et al.* (2011) with slight modifications as described below. Gall sections were incubated with blocking buffer (1% BSA in PIPES buffer pH 6.9) at RT for 2 hrs. The Mg16820 specific AB was diluted to 1:100 in fresh blocking solution and 200 µl were placed on each slide. As a negative control, the pre-immune serum was diluted 100 times in fresh blocking solution and 200 µl were added on each slide. Dilutions containing the AB or pre-immune serum were incubated for 1 h at 37°C and centrifuged for 5 min. As another negative control, slides were only treated with secondary AB. All slides were incubated in a humid box at 4°C overnight and prior to incubation with the secondary AB placed at 37°C for 1 h and washed for 30 min in 50 mM Pipes buffer. Subsequently, slides were incubated with the secondary AB (Goat anti-Rabbit IgG (H+L) Alexa Fluor 488, ThermoFisher Scientific), diluted 1:300 in blocking solution and incubated at 37°C for 2 hrs. The slides were washed in PIPES buffer for 30 min. To stain the nuclei, slides were incubated in 1.0 µg/ml 4’,6-diamidino-2-phenylindole (DAPI) for 1 min at RT, rinsed in distilled water, mounted in 90% glycerol and coverslipped. Sections were observed with a fluorescence microscope (Zeiss) and imaged. Autofluorescence (reddish signal) and

Alexa-488 (green) fluorescence were distinguished using a double band pass filter (Zeiss). In addition differential interference contrast transmission and DAPI-stained DNA images were obtained to obtain overlaid images.

Subcellular localization

Agrobacterium tumefaciens strain GV3101 carrying the construct of *Mg16820* fused to the *eGFP* tag C- or N- terminally or *eRFP* tag C- or N- terminally were suspended in infiltration buffer (IB) to an OD_{600} of 0.01 and used for infiltration in *N. benthamiana* leaves as described above. The same was done for *Mg16820* fused to it native signal peptide and the *eGFP* tag N-terminally. As a control a pK7WG2 derivative for expression of *eGFP* or *eRFP* was used. Infiltrated plants were kept in daylight at RT and 48 hrs after inoculation infiltrated spots were imaged using a confocal laser-scanning microscope (Nikon Instruments Inc., Tokyo, Japan). eGFP was excitated with a wavelength of 488 nm and emission was detected at 495-530 nm, eRFP was excitated with a wavelength of 561 nm and emission was detected at 592-632 nm. Auto-fluorescence of chlorophyll was collected at 657-737 nm.

Assay for reactive oxygen species (ROS) produced after flg22 incubation

Agrobacterium carrying *Mg16820* with or without its native signal peptide under control of the 35S promoter (vector pK7WG2) was grown in the dark for two days at 28°C in LB medium with 25 µg/ml rifampicin, 25 µg/ml gentamicin and 50 µg/ml spectinomycin. As negative control a plasmid with either a non-suppressing putative effector (*Mg03015*; contig03015 in Haegeman *et al.* (2013), no suppression of flg22 induced ROS production in more than three assays, unpublished data) with or without signal peptide was used. The aphid (*Myzus persicae*) effector *Mp10* was used as positive control (Bos *et al*., 2010). Before infiltration the agrobacteria were washed and diluted in IBto an optical density OD_{600} of 0.3 and incubated overnight slowly shaking in the dark at RT.

Nicotiana benthamiana leaves of 5-6 week old plants were infiltrated with Agrobacteria using a needleless syringe. Prior to infiltration a small hole was made on the abaxial site of the leaf with a needle. The agrobacteria holding the above mentioned constructs were infiltrated at different spots on the same leaf. Per assay one leaf of 8 plants was used with two replicates per spot. Circa 30 hrs after infiltration 16 mm^2 leaf discs were collected from the infiltrated areas with a cork borer and transferred to 96-well plates and floated overnight on 190 µL filter sterilized ultrapure water for recovery. After 48 hrs the water was removed and replaced by a mixture of 100 nM flg22 (QRLSSGLRINSAKDDAAGLAIS (Felix *et al*., 1999)), 0.5 mM luminol probe 8-amino-5-chloro-7-phenyl-pyrido[3,4-d]pyridazine-1,4(2H,3H)dione (L-012) (Wako Chemicals USA) and 20 µg/ml horseradish peroxidase (Sigma). The ROS production was measured by a luminol-based assay (Keppler *et al*., 1989) during 60 min. with measurements every 46 seconds with integration at 750 ms. For *Mg16820* both with (*SPMg Mg16820)* or without predicted signal peptide (*Mg Mg16820)* the assay was repeated more than three times. Student's T-test was used to determine significant differences per time point.

Effector triggered immunity assay (ETI)

ETI assays with several combinations of resistance/avirulence (*R/Avr)* genes were co-infiltrated with *Mg16820* either with (*SPMg16820)* or without (*Mg16820)* predicted signal peptide to test for its capacity to suppress the HR. The *R/Avr* pairs used for induction of a hypersensitive response (HR) were *R2/Avr2* (Saunders *et al*., 2012), *R3a/Avr3aKI* 32 (Armstrong *et al*., 2005), *Gpa2/RBP-1* (Sacco *et* *al*., 2009) *Cf-4/Avr4* and *Cf-9/Avr9* (Thomas *et al*., 2000). Furthermore, *Mi-1.2*^{T557S} the auto-active form of *Mi-1.2* (Gabriëls *et al.*, 2007) and the PAMP elicitor *INF1* (Kamoun *et al*., 2003) were included. *Agrobacterium tumefaciens* strain GV3101 was used for transformation as described above. Two negative controls were included in the suppression assay, GV3101 without construct or with pK7WG2-*GFP*. Agrobacteria carrying a plasmid for *Mg16820* expression or for expression of *R/Avr* genes were grown for 2-3 days in 10 ml LB medium with the appropriate antibiotics. Before infiltration the cells were pelleted and washed and resuspended in IB and incubated for at least 3 hrs at RT. Depending on the combination of constructs, the final concentration in the mixtures was adjusted to an OD_{600} of 0.5 or 0.6 for *Mg16820*and 0.5 or 0.4 for the *R* and *Avr* genes. The mixtures were spot infiltrated in *N. benthamiana* leaves of 5-6 weeks old plants as described before with negative controls on the same leaf as the tested effector. Per plant two leaves were infiltrated and 20 plants were used per assay. When a HR started to appear, the response was recorded for 2 or 3 days until almost all control spots resulted in an HR. HR on a spot was considered as suppressed when less than 50% of that spot showed cell death following the method of Gilroy *et al.* (2011). Fisher's exact test was used to statistically analyze the results. Each assay was performed at least twice and combinations showing suppression were repeated at least three times.

Yeast two-hybrid screening

A yeast two-hybrid screen was performed using the ProQuest system (Invitrogen). The pDEST32-*Mg16820* and empty pDEST22 were co-infiltrated in the yeast strain MaV103 to test auto-activation on SC-Leu-Trp-His (-TLH) -medium supplemented with 10 mM 3-Amino-1,2,4-triazole to screen for *HIS3* expression, SC-Leu-Trp-Ura medium for *URA3* expression (-TLU) and for expression of the *lacZ* reporter gene (X-gal). A commercially synthesized cDNA library of pathogen infected rice tissue was cloned in vector pDEST22 (Invitrogen). The rice tissue was a collection of root tissue infected with *M. graminicola* and *Hirschmanniella oryzae* at several time points as well as root and leaf tissue infected with fungi. The screening was repeated three times resulting in at least 1,000,000 transformants in each screen. Plasmids were extracted from colonies obtained on -TLH selection medium and they were cloned in *E. coli*. Plasmid preps were sequenced (LGC genomics) and one prey was found in frame. This prey was co-transformed with *Mg16820* in pDEST32 to confirm the positive result. The complete coding sequence of the host protein was picked up from leaf tissue cDNA rice using gene specific primers (DIP1-FL-F and DIP1-FL-R). *DIP1* without start codon was cloned as described above and ligated in the pDEST22 and pDEST32 vectors and co-transformed with *Mg16820* in pDEST32 and pDEST22 respectively. Colonies obtained from SC-Leu-Trp (–TL) plates were further analyzed compared to the auto-activation test.

Bimolecular fluorescence complementation

Mg16820 was cloned in vector pCL113 (YFPc:: Mg16820) and the gene for the potential target protein DIP1 was cloned in pCL112 (YFPn::DIP1). As a negative control, a putative effector (*Mg03015*, described above) with similar protein size and subcellular localization was cloned in vector pCL113. Constructs were transformed in *A. tumefaciens* strain GV3101 and complementary constructs were co-infiltrated in *N. benthamiana* leaves at OD_{600} in 4 different final concentrations: 0.01, 0.03, 0.1 and 0.3. YFP signal was analyzed 48 hrs after infiltration. YFP was excited with a wavelength of 514 nm and emission collected at 530-575 nm using confocal microscopy (Nikon Instruments Inc., Tokyo, Japan).

RNA extraction from leaves

To compare expression of *Mg16820* and the negative control putative effector *Mg03015* used in the bimolecular fluorescence complementation, RNA extraction was done by grinding 0.2 g infiltrated *N. benthamiana* leaf tissue in liquid nitrogen and RNA extraction was performed following the protocol of RNeasy Mini Kit (Qiagen). RNA was treated with DNAseI, checked on the presence of gDNA and then used as template for cDNA synthesis (3 μg in 36 μL reaction mix) (tetro cDNA synthesis kit, Bioline). Semi-quantitative PCR was performed with primers targeting cDNA of the house-keeping gene *elongation factor 1a* (EF1α-F and EF1α-R) (supplementary data, Liu *et al.,* 2012) to normalize the cDNA template. Primers 52FNew and 52RNew and for the negative control 50FNew and 50RNew were used for detection of the effector mRNA (supplementary data). As PCR template, 5 μL of cDNA mix was used in 40 μL PCR mix. At 25, 30 and 35 PCR cycles, 10 μL of PCR mix was withdrawn from the PCR mix and loaded on gel to analyze the results. 35 PCR cycles was repeated in 30 μL PCR mix and loaded on gel to normalize *Mg03015*/*Mg16820* expression to *elongation factor 1a* expression.

Acknowledgements

The authors would like to acknowledge the Research Foundation Flanders FWO for financial support (FWO grants G010712N and 1502312N) and the Special Research Fund of Ghent University for the BOF13/GOA/030 project.

The authors also thank Lien De Smet for technical support and Dr. John Jones for hosting Dr. Annelies Haegeman at the James Hutton Institute (Dundee, UK) and Dr. Miles Armstrong for teaching the yeast two-hybrid protocol during that stay, funded by COST Action 872 (COST-STSM-872-6657). The visit to INRA to perform the immunolocalization was funded by COST Action SUSTAIN FA1208.

References

Abad, P., Favery, B., Rosso, M. N. and Castagnone-Sereno, P. (2003). Root-knot nematode parasitism and host response: Molecular basis of a sophisticated interaction. *Molecular Plant Pathology* 4(4), 217–224. DOI: 10.1046/j.1364-3703.2003.00170.x

Ali, S., Magne, M., Chen, S., Côté, O., Stare, B.G., Obradovic, N., Jamshaid, L., Wang, X., Bélair, G., Moffett, P. (2015). Analysis of putative apoplastic effectors from the nematode, *Globodera rostochiensis*, and identification of an expansin-like protein that can induce and suppress host defenses. *Public Library of Science one* 10(1), 1–23. DOI: 10.1371/journal.pone.0115042.

Ali, M.A. Azeem, F., Li, H. and Bohlmann, H. (2017). Smart parasitic nematodes use multifaceted strategies to parasitize plants. *Frontiers in Plant Science* 8, 1699. DOI: 10.3389/fpls.2017.01699

de Almeida Engler, J., Van Poucke, K., Karimi, M., De Groodt, R., Gheysen, G., Engler, G. and Gheysen, G. (2004). Dynamic cytoskeleton rearrangements in giant cells and syncytia of nematode-infected roots. *Plant Journal* 38 pp.12-26. DOI: 10.1111/j.1365-313X.2004.02019.x

Armstrong, M. R., Whisson, S. C., Pritchard, L., Bos, J. I. B., Venter, E., Avrova, A.,Rehmany, A.P., Bohme, U., Brooks, K., Cherevach, I. Hamlin, N., White, B., Fraser, A., Lord, A., Quail, M.A., Churcher, C., Hall, N., Berriman, M., Huang, S., Kamoun, S., Beynon, J.L. and Birch, P.R.J. (2005). An ancestral oomycete locus contains late blight avirulence gene Avr3a, encoding a protein that is recognized in the host cytoplasm. *Proceedings of the National Academy of Sciences of the USA* 102, 7766–7771.

Asselbergh, B., Vleesschauwer, D. and Höfte, M. (2008). Global switches and fine-tuning-ABA modulates plant pathogen defense. *Molecular Plant-Microbe Interactions* 21(6), 709–719. DOI: 10.1094/ MPMI -21-6-0709

Baermann (1917). Eine einfache Methode zur Auffindung von Ankylostomum -(Nematoden)- Larven in Erdproben. *Mededelingen uit het Geneeskundig Laboratorium te Weltevreden*, 41–47.

Blanc-Mathieu, R., Perfus-Barbeoch, L., Aury, J., Da Rocha, M., Gouzy, J., Sallet, E., Martin-Jimenez, C., Bailly-Bechet, M., Castagnone-Sereno, P., Flot, J., Kozlowski, D.K., Cazareth, J., Couloux, A., Da Silva, C., Guy, J., Kim-Jo, Y., Rancurel, C., Schiex, T., Abad, P., Wincker, P. and Danchin, E.G.J. (2017). Hybridization and polyploidy enable genomic plasticity without sex in the most devastating plant-parasitic nematodes. *PLoS Genetics* 13(6). DOI: e1006777

de Boer, J.M., Yan, Y., Smant, G., Davis, E.L. and Baum, T.J. (1998). *In-situ* hybridization to messenger RNA in *Heterodera glycines*. *Journal of Nematology* 30(3), 309-312.

Bos, J.I., Prince, D., Pitino, M., Maffei, M.E., Win, J. and Hogenhout, S.A. (2010). A functional genomics approach identifies candidate effectors from the aphid species *Myzus persicae* (green peach aphid). *PLoS Genetics* 6 (11). DOI: 10.1371/journal.pgen.1001216.

Bridge, J., Plowright, R.A.and Peng, D. (2005). *Nematode parasites of rice*. In: Bridge, J., Coyne, D. L. and Kwoseh, C. K. (Eds). Nematode parasites of tropical root and tuber crops, plant parasitic nematodes in subtropical and tropical agriculture: second edition. CABI Bioscience, UK Centre, Bakeham Lane, Egham, Surrey TW20 9TY, UK, 87-130.

Chen, J., Lin, B., Huang, Q., Hu, L., Zhuo, K. and Liao, J. (2017). A novel *Meloidogyne graminicola* effector, MgGPP, is secreted into host cells and undergoes glycosylation in concert with proteolysis to suppress plant defenses and promote parasitism. *PLoS Pathogens* 13(4), 1–24. DOI: 10.1371/journal.ppat.1006301.

Chen, J., Hu, L., Sun, L., Lin, B., Huang, K., Zhuo, K. and Liao, J. (2018). A novel *Meloidogyne graminicola* effector, MgMO237, interacts with multiple host defense-related proteins to manipulate plant basal immunity and promote parasitism. Molecular Plant Pathology, accepted paper DOI: 10.1111/mpp.12671

Davis, E.L., Hussey, R.S., Baum, T.J., Bakker, J., Schots, A., Rosso, M.N., Abad, P. (2000). Nematode parasitism genes. *Annual Review of Phytopathology* 38, 365-396. DOI: 10.1146/annurev.phyto.38.1.365

Denancé, N. Sánchez-Vallet, A., Goffner, D. and Molina, A. (2013). Disease resistance or growth: the role of plant hormones in balancing immune responses and fitness costs. *Frontier in Plant Science* 4, 155. DOI: 10.3389/fpls.2013.00155

Felix, G. Duran, J.D., Volko, S., and Boller, T. (1999). Plants have a sensitive perception system for the most conserved domain of bacterial flagellin. *Plant Journal* 18(3), 265–276.

Gabriëls, S.H., Vossen, J.H., Ekengren, S.K., van Ooijen. G., Abd-El-Haliem, A.M., van den Berg, G.C., Rainey, D.Y., Martin, G.B., Takken, F.L., de Wit, P.J., and Joosten M.H. (2007). An NB-LRR protein required for HR signalling mediated by both extra- and intracellular resistance proteins. *Plant Journal* 50(1), 14–28. DOI: 10.1111/j.1365-313X.2007.03027.x

Gilroy, E.M., Taylor, R.M., Hein, I., Boevink, P., Sadanandom, A. and Birch, P.R. (2011). CMPG1-dependent cell death follows perception of diverse pathogen elicitors at the host plasma membrane and is suppressed by *Phytophthora infestans* RXLR effector AVR3a. *The New phytologist* 190(3), 653–66. DOI: 10.1111/j.1469-8137.2011.03643.x

Haegeman, A., Bauters, L., Kyndt, T., Rahman, M.M. and Gheysen, G. (2013). Identification of candidate effector genes in the transcriptome of the rice root knot nematode *Meloidogyne graminicola*. *Molecular plant pathology* 14(4), 379–90. DOI: 10.1111/mpp.12014

Hewezi, T. & Baum, T.J. (2013). Manipulation of plant cells by cyst and root-knot nematode effectors. *Molecular plant-microbe interactions* 26(1), 9–16. DOI: 10.1094/MPMI-05-12-0106-FI

Hoagland, D. R. and Arnon, D. I. (1950). The water-culture method for growing plants without soil. *Circular. California Agricultural Experiment Station* 347 (20), 32.

Holsters, M., de Waele, D., Depicker, A., Messens, E., Montagu, M.V. and Schell, J. (1978). Transfection and transformations of *Agrobacterium tumefaciens*. *Molecular & General Genetics* 163: 181-187.

Jaouannet, M. and Rosso, M.N., 2013. Effectors of root sedentary nematodes target diverse plant cell compartments to manipulate plant functions and promote infection. *Plant signaling & behavior* 8(9), 1–5. DOI: 10.4161/psb.25507

Ji, H., Kyndt, T., He, W., Vanholme, B. and Gheysen, G. (2015). β-aminobutyric acid-induced resistance against root-knot nematodes in rice is based on increased basal defense. *Molecular plant-microbe interactions* 28(5), 519–533. DOI: 10.1094/MPMI-09-14-0260-R

Jones, J.D.G. and Dangl, L., (2006). The plant immune system. *Nature* 444, 323–329. DOI:10.1038/nature05286

Jwa, N.S. and Hwang, B.K. (2017). Convergent evolution of pathogen effectors toward reactive oxygen species signaling networks in plants. *Frontiers in Plant Science* 8, 1–12. DOI: 10.3389/fpls.2017.01687

Kamoun, S., Hamada, W., & Huitema, E. (2003). Agrosuppression : a bioassay for the hypersensitive response suited to high-throughput screening. *Molecular Plant-Microbe Interactions* 16(1), 7–13. DOI: 10.1094/MPMI.2003.16.1.7

Kavitha, P.G., Umadevi, M., Suresh, S. and Ravi, V., 2016. The rice root-knot nematode (*Meloidogyne graminicola*) - life cycle and histopathology. *International journal of science and nature* 7(3), 483-486. DOI: 10.1163/15685411-00002746

Keppler, L. D., Baker, C. J., and Atkinson, M. M. (1989). Active oxygen production during a bacteria-induced hypersensitive reaction in tobacco suspension cells. *Phytopathology* 79, 974-978.

Kronenberger, J., Desprez, T., Höfte, H., Caboche, M. and Traas, J. (1993). A methacrylate embedding procedure developed for immunolocalization on plant tissues is also compatible with *in situ* hybridization. Cell biology international 17(11), 1013–1021. DOI: 10.1006/cbir.1993.1031

Kyndt, T., Fernandez, D. and Gheysen, G. (2014). Plant-parasitic nematode infections in rice: molecular and cellular insights. *Annual review of phytopathology* 52, 135–153. DOI: 10.1146/annurev-phyto-102313-050111

Kyndt, T., Nahar, K., Haeck, A., Verbeek, R., Demeestere, K., and Gheysen, G., (2017). Interplay between carotenoids, abscisic acid and jasmonate guides the compatible rice-*Meloidogyne graminicola* interaction. *Frontiers in Plant Science* 8, 1–11. DOI: 10.3389/fpls.2017.00951

Lievens, L. Pollier, J., Goossens, A., Beyaert, R. and Staal, J. (2017). Abscisic acid as pathogen effector and immune regulator. *Frontiers in Plant Science* 8, 1–15. DOI: 10.3389/fpls.2017.00587

Lin J.R., Mondal, A.M., Liu, R. and Hu, J. (2012). Minimalist ensemble algorithms for genome-wide protein localization prediction. BMC Bioinformatics 13:157 DOI: 10.1186/1471-2105-13-157.Liu, D. Shi, L., Han, C., Yu, J., Li, D. and Zhang, Y. (2012). Validation of reference genes for gene expression studies in virus-infected *Nicotiana benthamiana* using quantitative real-time PCR. *Public Library of Science one* 7(9). DOI: 10.1371/journal.pone.0046451

Mantelin, S. Bellafiore, S. and Kyndt, T. (2017). Pathogen profile *Meloidogyne graminicola*: a major threat to rice agriculture. *Molecular Plant Pathology* 8, 3–15. DOI: 10.1111/mpp.12394

Manosalva, P., Manohar, M., von Reuss, S.H., Chen, S., Koch, A., Kaplan, F., Choe, A., Micikas, R.J., Wang, X., Kogel, K., Sternberg, P.W., Williamson, V.M., F.C., Schroeder and Klessig, D.F. (2015). Conserved nematode signalling molecules elicit plant defenses and pathogen resistance. *Nature Communications* 6, 7795. DOI: http://dx.doi.org/10.1038/ncomms8795.

Niu, J., Liu, P., Liu, Q., Chen, C., Guo, Q., Yin, J., Yang, G. and Jian, H. (2016). Msp40 effector of root-knot nematode manipulates plant immunity to facilitate parasitism. *Scientific reports* 6, 19443. DOI: 10.1038/srep19443.

Nguyen, C.N., Perfus-Barbeoch, L., Quentin, M., Zhao, J., Magliano, M., Marteu, N., Da Rocha, M., Nottet, N., Abad, P. and Favery, B. (2018). A root-knot nematode small glycine and cysteine-rich secreted effector, MiSGCR1, is involved in plant parasitism. *New Phytologist* 217, 687–699. DOI: 10.1111/nph.14837.

Petitot, A.S., Dereeper, A., Agbessi, M., Da Silva, C., Guy, J., Ardisson, M. and Fernandez, D. (2016). Dual RNA-seq reveals *Meloidogyne graminicola* transcriptome and candidate effectors during the interaction with rice plants. *Molecular Plant Pathology*, 17(6), 860–874. DOI: 10.1111/mpp.12334.

Qi, J., Wang, J., Gong, Z. and Zhou, J. (2017). Apoplastic ROS signaling in plant immunity. *Current Opinion in Plant Biology* 38, 92-100. DOI: 10.1016/j.pbi.2017.04.022

Reversat, G. and Boyer, J. (1999). A mixture of sand and water-absorbent synthetic polymer as substrate for the xenic culturing. *Nematology* 1(2), 209–212.

Sacco, M.A. Koropacka, K., Grenier, E., Jaubert, M.J., Blanchard, A., Goverse, A., Smant, G. and Moffett, P. (2009). The cyst nematode SPRYSEC protein RBP-1 elicits Gpa2- and RanGAP2-dependent plant cell death. *PLoS Pathogens* 5(8). DOI:10.1371/journal.ppat.1000564.

Saleh, A., Lumbreras, V., Lopez, C., Dominguez-Puigjaner, E., Kizis, D. and Pagès, M. (2006). Maize DBF1-interactor protein 1 containing an R3H domain is a potential regulator of DBF1 activity in stress responses. *Plant Journal* 46(5), 747-57.

Saunders, D.G.O., Breen, S., Win, J., Schornack, S., Hein, I., Bozkurt, T.O., Champouret, N., Vleeshouwers, V.G.A.A., Birch, P.R.J., Gilroy, E.M. and Kamoun, S. (2012). Host protein BSL1 associates with *Phytophthora infestans* RXLR effector AVR2 and the *Solanum demissum* immune receptor R2 to mediate disease resistance. *The Plant Cell* 24(8), 3420–3434.

Smant, G., Stokkermans, J.P.W.G., Yan, Y., De Boer, J.M., Baum, T.J., Wang, X., Hussey, R.S., Gommers, F.J., Henrissat, B., Davis, E.L., Helder, J., Schots, A. and Bakker, J., (1998). Endogenous cellulases in animals: Isolation of -1,4-endoglucanase genes from two species of plant-parasitic cyst nematodes. *Proceedings of the National Academy of Sciences* 95(9), 4906–4911. DOI: 10.1073/pnas.95.9.4906

Sperschneider, J., Catanzariti, A.M., DeBoer, K., Petre, B., Gardiner, D.M., Singh, K.B., Dodds, P.N. and Taylor, J.M. (2017). LOCALIZER: subcellular localization prediction of both plant and effector proteins in the plant cell. Scientific Reports 7:44598. DOI: 10.1038/srep44598

Thomas, C.M., Tang, S., Hammond-kosack, K. and Jones, J.D.G. (2000). Comparison of the hypersensitive response induced by the tomato Cf-4 and Cf-9 genes in *Nicotiana* spp . *Molecular Plant-Microbe Interactions* 13(4), 465–469. DOI: 10.1094/MPMI.2000.13.4.465

Torres, M.A., Jones, J.D. and Dangl, J.L. (2006). Reactive oxygen species signaling in response to pathogens. *Plant physiology* 141(2), 373–378. DOI: 10.1104/pp.106.079467

Vieira, P., Danchin, E.G.J., Neveu, C., Crozat, C., Jaubert, S., Hussey, R.S., Engler, G., Abad, P., de Almeida-Engler, J., Castagnone-Sereno, P. and Rosso, M. (2011). The plant apoplasm is an important recipient compartment for nematode secreted proteins. *Journal of experimental botany* 62(3), 1241–53. DOI: 10.1093/jxb/erq352

Vilardell, J., Goday, A., Freire, M.A., Torrent, M., Martínez, M.C., Torné, J.M. and Pagès, M. (1990). Gene sequence, developmental expression, and protein phosphorylation of RAB-17 in maize. *Plant Molecular* Biology 14(3), 423-32.

Wang, R. and Brattain, M.G. (2007). The maximal size of protein to diffuse through the nuclear pore is larger than 60 kDa. FEBS Letters 581(17), 3164–3170. DOI: 10.1016/j.febslet.2007.05.082

Yik, C. and Birchfield, W. (1979). Host studies and reactions of rice cultivars to *Meloidogyne graminicola*. *Phytopathology* 69 (5), 497-499. DOI: 10.1094/Phyto-69-497

Supplementary Material

Table S1. Primers used in this study

Primer	Sequence 5'- 3'	Purpose
Mg16820-F-FL	GGGGGATTCACCTTAAACAAC	PCR coding region for ligation in vector p-GEMT
Mg16820-R-FL	CTCGTGTAGCTTCTTTAATGC	
Mg16820-attb1+start	aaaaagcaggcttaATGGGGAGAAAAAAGGG	Adding attb site for cloning in pDONR221
Mg16820-attb1	aaaaagcaggcttaGGGAGAAAAAAGGG	
Mg16820-SP-attb1+start	aaaaagcaggcttaATGTCGAAATTCCTTATTGTTCTTG	
Mg16820-SP-attb1:	aaaaagcaggcttaTCGAAATTCCTTATTGTTCTTG	
Mg16820-attb2+stop:	agaaagctgggtgTTACTGTCCAATCATCCTTTGAAAATC	
Mg16820-attb2:	agaaagctgggtgCTGTCCAATCATCCTTTGAAAATC	
Mg16820SP-eff-F:	TCGAAATTCCTTATTGTTCTTG	Colony PCR, RT-PCR
Mg16820 Fnew	AAAAAGGGTGTTCCCCAAC	
Mg16820 Rnew	CCAATCATCCTTTGAAAATCG	
Mg16820-F-ISH	GGGGGATTCACCTTAAACAA	*In situ* hybridization
Mg16820-R-ISH	CCAATCATCCTTTGAAAATCG	
Mg03015-F-FL	CTCCTTTGAAAATGGCTAAAATC	PCR coding region for ligation in vector p-GEMT
Mg03015-R-FL	CTTTTCTTTATATACTTGAACTTC	PCR coding region for ligation in vector p-GEMT
Mg03015-SP-attb1+start	aaaaagcaggcttaATGGCTAAAATCAATTTTATAAAATTTATTC	Adding attb site for cloning in pDONR221
Mg03015-attb1	aaaaagcaggcttaGGTTCAGATGAAGTTGAG	
Mg03015-attb2+stop:	agaaagctgggtgTTAATTTACTTGGAGTCCCAATCG	
Mg03015 Fnew	TTCAGATGAAGTTGAGCCACA	Colony PCR, RT-PCR
Mg03015 Rnew	TTACTTGGAGTCCCAATCGA	
Mg9152-F-ISH	GACATGAACAGAAGCGTCCA	*In situ* hybridization
Mg9152-R-ISH	AGCGGCAACATTGGTTACTT	
DIP1-FL-F	ATGAGCTCCGGCGCCGCCTC	PCR coding region for ligation in vector p-GEMT
DIP1-FL-R	TCAGCCATGGTTGAAGGACT	
DIP1-attb1	aaaaagcaggcttaAGCTCCGGCG	Adding attb site for cloning in pDONR221
DIP1-attb2+stop	agaaagctgggtgTCAGCCATGGTTGAAGGACT	
EF1α-F	GGTATTCTCAAACCTGGAATGG	*N. benthamiana* housekeeping gene for RT-PCR
EF1α-R	AACATTGTCACCAGGAACAGC	*N. benthamiana* housekeeping gene for RT-PCR
SP6	ATTTAGGTGACACTATAGAATACTCAAGC	Primer used for sequencing pGEM-T constructs
T7	TAATACGACTCACTATAGGGCGAATTGG	
attB1	ACAAGTTTGTACAAAAAAGCA	pDONR221 insert
attB2	ACCACTTTGTACAAGAAAGCT	
M13-F	GTAAAACGACGGCCAG	Primer used for sequencing pDONR221 constructs
M13-R	CAGGAAACAGCTATGAC	
35S fragment F	GAAACCTCCTCGGATTCCAT	several destination vectors
pCL112-NYFP-F	CAACTACAACAGCCACAACG	Primer used for sequencing pCL112 constructs
pCL113-CYFP-F	CCGACAACCACTACCTGAG	Primer used for sequencing pCL113 constructs
pDEST-R	AGCCGACAACCTTGATTGGAGAC	Primer used for sequencing pDEST22, pDEST32 constructs

>Contig16820
GGGGGATTCACCTTAAACAACTCTAAAAAATACTTTGAATTAAACAAAAA**ATG**TCGAAATTCCTTATT
GTTCTTGTAATTTTTATTTTTGTTTTTATTGAGAGTTCTAATGCTGGGAGAAAAAAGGGTGTTCCCCA
ACGAGCACCTAGAGGCGATATAGGAGATGATAAAAGACATGCACAAACGGATCACGGAAAGGATAGTG
ATTCTTATGGTAATTCTAATGGTGGTTCTTATGGTTCAGCTAACTCATTTGGAGCTCATGGACAATGC
GATCATATACCTAGAGAAGAGCTCGATTTTCAAAGGATGATTGGACAG**TAA**AAGCATTAAAGAAGCTA
CACGAGT

MSKFLIVLVIFIFVFIESSNAGRKKGVPQRAPRGDIGDDKRHAQTDHGKDSDSYGNSNGGSYGSANSFGAHGQCD
HIPREELDFQRMIGQ*

Fig. S1 cDNA and protein sequence of Mg16820. Start and stop codons are shown in bold. The predicted signal peptide is underlined.

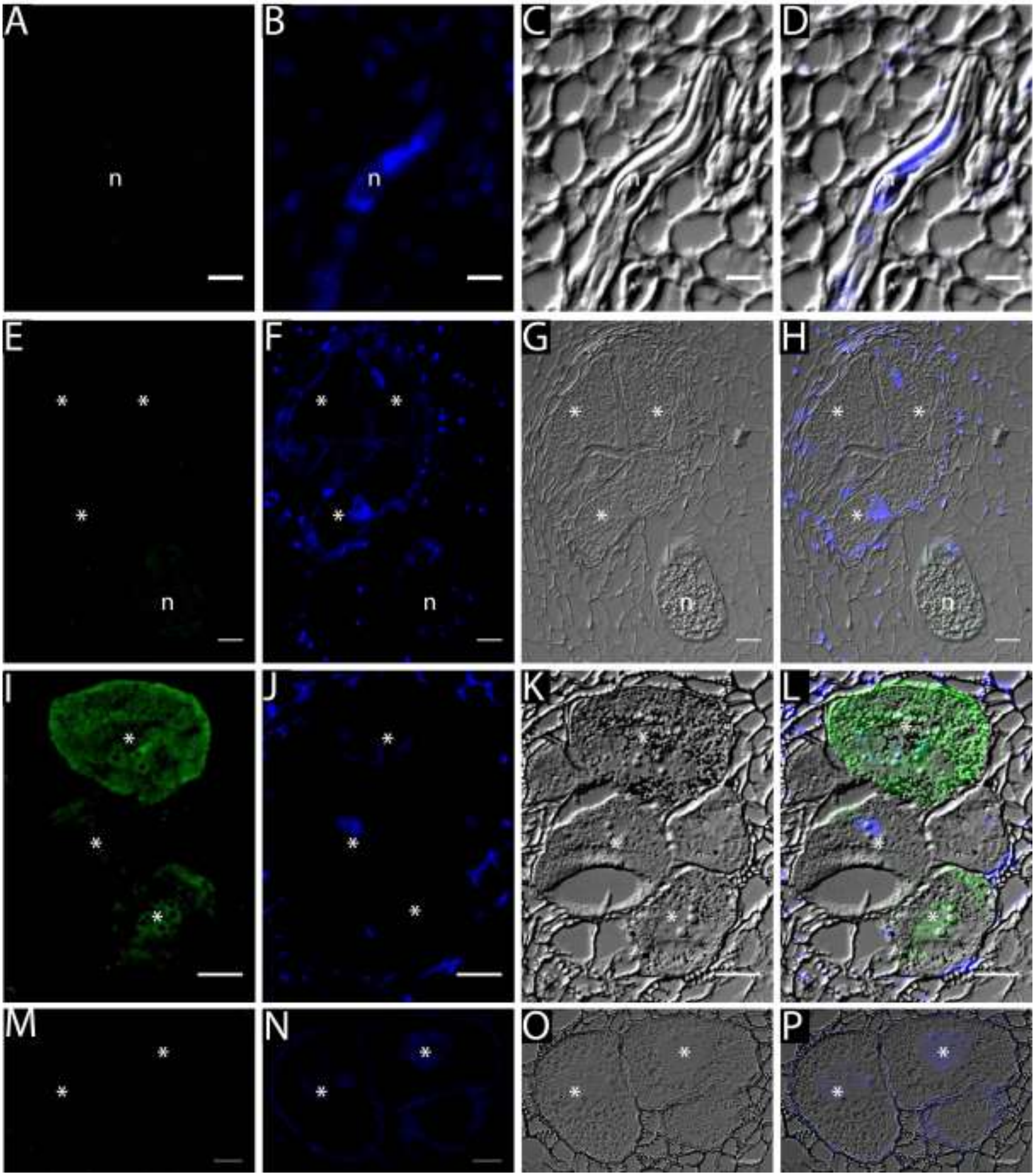

Fig. S2 Immunodetection of the effector Mg16820 in sectioned rice galls. (A–D) Migratory nematodes incubated with pre-immune serum, showing no signal. (E–H) Galls and nematode at 5 days post-inoculation (dai) incubated with pre-immune serum, showing no signal. (I–L) Galls at 7 dai incubated with primary and secondary antibody, showing signal in the cytoplasm. (M–P) Galls at 10 dai incubated with primary and secondary antibody, showing no signal. (A, E, I, M) Detection of Alexa Fluor 488-conjugated secondary antibody. (B, F, J, N) Detection of 4′,6-diamidino-2-phenylindole (DAPI)-stained nuclei. (C, G, K,

O) Images of differential interference contrast (DIC). (D, H, L, P) DIC, DAPI and green fluorescent protein (GFP) overlay. n, nematode; asterisks, giant cells. Scale bars: (A–D) 10 µm; (E–P) 20 µm.

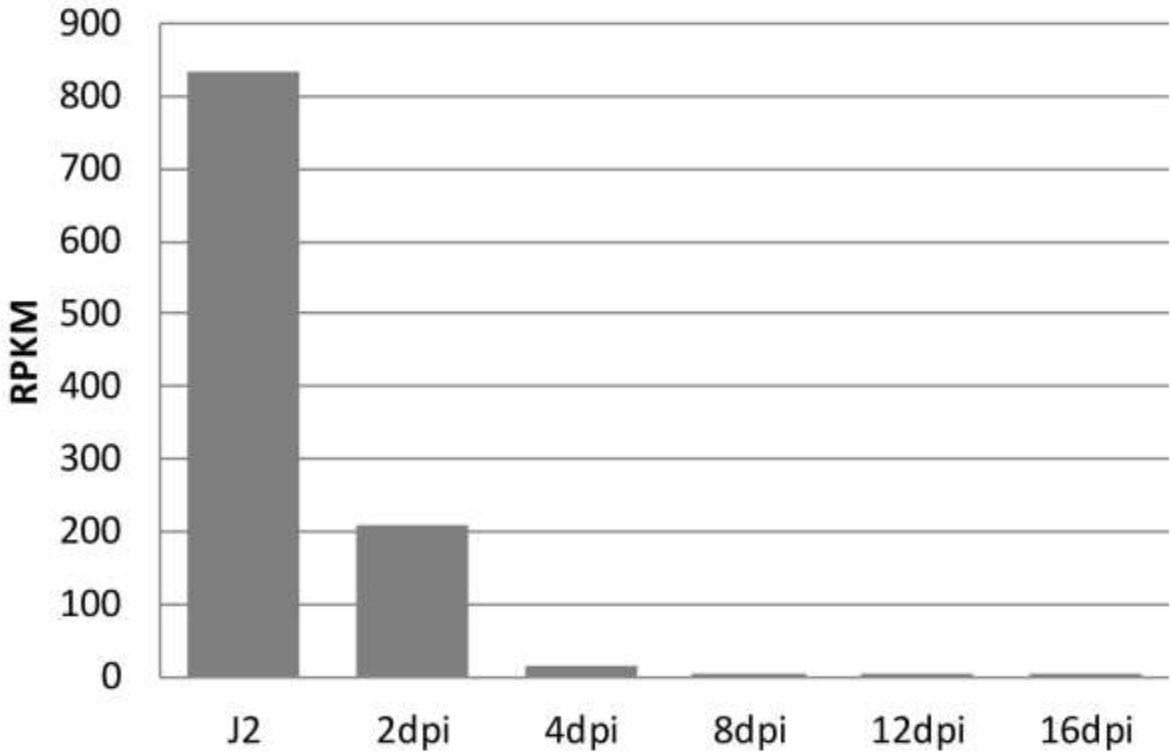

Fig. S3 Reverse transcription-polymerase chain reaction (RTPCR) to compare the expression of Mg16820 (YFPc::Mg16820) and Mg03015 (YFPc::Mg03015) in *Nicotiana benthamiana* leaves with the housekeeping gene elongation factor 1α(EF1α) as control. (A) Expression of EF1α in Mg03015 sample. (B) Expression of EF1α in Mg16820 sample (182 bp). Expression of Mg03015 in (C) is similar to expression of Mg16820 (198 bp) in (D). Result after 35 PCR cycles.

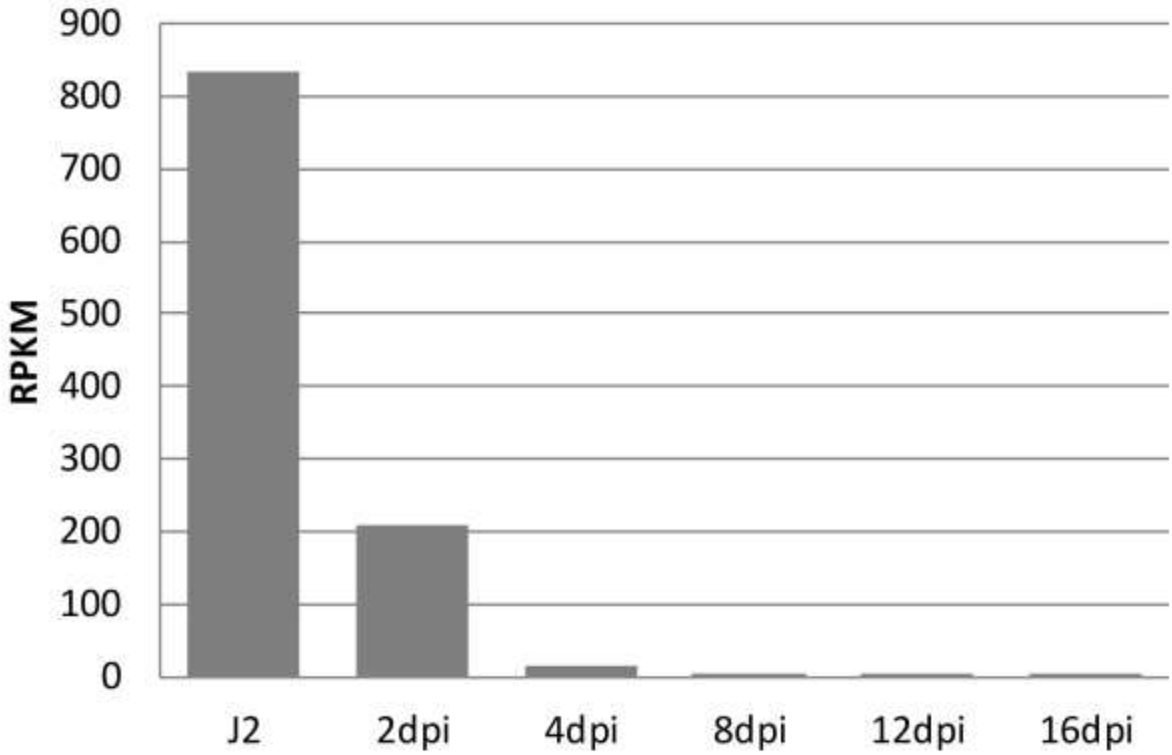

Fig. S4 Expression of Mg16820 in pre-parasitic second-stage juveniles (J2s) and at different time points in root tissue. RNA sequencing results in reads per kilobase million (RPKM). Results present the average of two replicates.